



1 Volatility of mixed atmospheric Humic-like Substances and ammonium sulfate particles

2 Wei Nie^{1,2,3,8*}, Juan Hong³, Silja A. K. Häme³, Aijun Ding^{1,2,8*}, Yugen Li⁴, Chao Yan³, Liqing Hao⁵,
3 Jyri Mikkilä³, Longfei Zheng^{1,2,8}, Yuning Xie^{1,2,8}, Caijun Zhu^{1,2,8}, Zheng Xu^{1,2,8}, Xuguang Chi^{1,2,8}, Xin
4 Huang^{1,2,8}, Yang Zhou^{6,7}, Peng Lin^{6,a}, Annele Virtanen⁵, Douglas R. Worsnop³, Markku Kulmala³,
5 Mikael Ehn³, Jianzhen Yu⁶, Veli-Matti Kerminen³ and Tuukka Petäjä^{3,1}

6 ¹ Joint International Research Laboratory of Atmospheric and Earth System Sciences, Nanjing University,
7 Nanjing, China

8 ² Institute for Climate and Global Change Research & School of Atmospheric Sciences, Nanjing University,
9 Nanjing, 210023, China

10 ³ Division of Atmospheric Sciences, Department of Physics, University of Helsinki, Helsinki, Finland

11 ⁴ Division of Environment, Hong Kong University of Science and Technology, Clear Water Bay, Kowloon,
12 Hong Kong, China

13 ⁵ Department of Applied Physics, University of Eastern Finland, Kuopio 70211, Finland

14 ⁶ Department of Chemistry, Hong Kong University of Science & Technology, Clear Water Bay, Kowloon, Hong
15 Kong, China

16 ⁷ Key Laboratory of Physical Oceanography, College of Oceanic and Atmospheric Sciences, Ocean University
17 of China, Qingdao 266100, China

18 ⁸ Collaborative Innovation Center of Climate Change, Jiangsu province, China

19 ^a now at: Environmental Molecular Sciences Laboratory, Pacific Northwest National Laboratory, Richland, WA
20 99532

*Correspondence to: A. J. Ding (dingaj@nju.edu.cn) and W. Nie (niewei@nju.edu.cn)

21 Abstract

22 The volatility of organic aerosols remains poorly understood due to the complexity of speciation and
23 multi-phase processes. In this study, we extracted HUMic-Like Substances (HULIS) from four
24 atmospheric aerosol samples collected at the SORPES station in Nanjing, eastern China, and
25 investigated the volatility behavior of particles at different sizes using a Volatility Tandem Differential



26 Mobility Analyzer (VTDMA). In spite of the large differences in particle mass concentrations, the
27 extracted HULIS from the four samples all revealed very high oxidation states ($O : C > 0.95$),
28 indicating secondary formation as the major source of HULIS in Yangtze River Delta (YRD). An
29 overall low volatility was identified for the HULIS samples, with the volume fraction remaining (VFR)
30 higher than 55% for all the re-generated HULIS particles at the temperature of 280 °C. A kinetic mass
31 transfer model was applied to the thermodenuder (TD) data to interpret the observed evaporation
32 pattern of HULIS, and to derive the mass fractions of semi-volatile (SVOC), low-volatility (LVOC)
33 and extremely low-volatility components (ELVOC). The results showed that LVOC and ELVOC
34 dominated (more than 80%) the total volume of HULIS. Atomizing processes led to a size dependent
35 evaporation of regenerated HULIS particles, and resulted in more ELVOCs in smaller particles. In
36 order to understand the role of interaction between inorganic salts and atmospheric organic mixtures in
37 the volatility of an organic aerosol, the evaporation of mixed samples of ammonium sulfate (AS) and
38 HULIS was measured. The results showed a significant but nonlinear influence of ammonium sulfate
39 on the volatility of HULIS. The estimated fraction of ELVOCs in the organic part of largest particles
40 (145 nm) increased from 26% in pure HULIS samples to 93% in 1:3 (mass ratio of HULIS:AS) mixed
41 samples, to 45% in 2:2 mixed samples, and to 70% in 3:1 mixed samples, suggesting that the
42 interaction tends to decrease the volatility of atmospheric organic molecular once condensing on
43 ammonium sulfate containing aerosols. Our results demonstrate that HULIS are important low volatile,
44 or even extremely low volatile, compounds in the organic aerosol phase. As important formation
45 pathways of atmospheric HULIS, multi-phase processes, including oxidation, oligomerization,
46 polymerization and interaction with inorganic salts, are indicated to be important sources of low
47 volatile and extremely low volatility species of organic aerosols.

48 1. Introduction

49 Atmospheric organic aerosol (OA) comprises 20-90% of the total submicron aerosol mass depending
50 on location (Kanakidou et al., 2005; Zhang et al., 2007; Jimenez et al., 2009), and play a critical role in
51 air quality and global climate change. Given the large variety of organic species, OA is typically
52 grouped in different ways according to its sources and physicochemical properties. These include the
53 classifications based on aerosol optical properties (brown carbon and non-light absorption OA),
54 formation pathways (primary (POA) and secondary (SOA) organic aerosol) and solubility (water
55 soluble OA (WSOA) and water insoluble OA (WISOA)). HUmic-Like Substances (HULIS), according



56 to their operational definition, are the hydrophobic part of WSOA, and contribute to more than half of
57 the WSOA (e.g. Krivácsy et al., 2008). Secondary formation (Lin et al., 2010b) and primary emission
58 from biomass burning (Lukács et al., 2007; Lin et al., 2010a) have been identified as the two major
59 sources of atmospheric HULIS. Because they are abundantly present, water-soluble, light-absorbing
60 and surface-active, HULIS in atmospheric particles have been demonstrated to play important roles in
61 several processes, including cloud droplet formation, light absorption and heterogeneous redox activities
62 (Kiss et al., 2005; Graber and Rudich, 2006; Hoffer et al., 2006; Lukács et al., 2007; Lin and Yu, 2011;
63 Verma et al., 2012; Kristensen et al., 2012).

64 Volatility of atmospheric organic compounds is one of their key physical properties determining their
65 partitioning between the gas and aerosol phases, thereby strongly influencing their lifetimes and
66 concentrations. Atmospheric OA can be divided into semi-volatile organic compounds (SVOC), low
67 volatility organic compounds (LVOC) and extremely low volatility organic compounds (ELVOC)
68 (Donahue et al., 2012; Murphy et al., 2014). LVOC and ELVOC are predominantly in the aerosol
69 phase and contribute largely to the new particle formation and growth (Ehn et al., 2014), while SVOC
70 have considerable mass fractions in both phases and usually dominate the mass concentration of OA.
71 As far as we know, volatility studies on OA have mostly focused on laboratory-generated organic
72 particles or ambient particles (Kroll and Seinfeld, 2008; Bilde et al., 2015). Laboratory-generated
73 organic particles contain only a small fraction of compounds present in atmospheric OA, whereas
74 ambient particles are usually complex mixtures of thousands of organic and several inorganic
75 compounds. One way to interlink laboratory and ambient studies, and to understand the volatility of
76 ambient OA systematically, might be to isolate some classes of OA from ambient particles before
77 investigating their volatility separately. As an important sub-group of organic aerosols in the real
78 ambient aerosols, the physicochemical properties of HULIS have been studied widely, including their
79 mass concentrations (Lin et al., 2010b), chemical composition (Lin et al., 2012; Kristensen et al., 2015;
80 Chen et al., 2016), density (Dinar et al., 2006) and hygroscopicity (Wex et al., 2007; Kristensen et al.,
81 2014). However, to the best of our knowledge, the volatility of atmospheric HULIS has never been
82 reported so far.

83 In the ambient aerosol, organic aerosol (OA, including HULIS) mostly co-exist with inorganic
84 compounds, such as ammonium sulfate. The volatility of OA has been demonstrated to be affected by
85 aerosol-phase reactions when mixed with inorganic compounds (Bilde et al., 2015). The most typical



86 examples of these are interactions between particulate inorganic salts with organic acids to form
87 organic salts, which evidently can enhance the partitioning of organic acids onto the aerosol phase
88 (Zardini et al., 2010; Laskin et al., 2012; Häkkinen et al., 2014; Yli-Juuti et al., 2013;). Recent studies
89 have reported that the saturation vapor pressure (p_{sat}) of ammonium oxalate is significantly lower than
90 that of pure oxalic acid, with p_{sat} being around 10^{-6} Pa for ammonium oxalate (Ortiz-Montalvo et al.,
91 2014; Paciga et al., 2014). However, this has not shown to be the case for adipic acid vs. ammonium
92 adipate, indicating that not all dicarboxylic acids react with ammonium to form low-volatility organic
93 salts (Paciga et al., 2014). Given that HULIS contain acidic species (Paglione et al., 2014; Chen et al.,
94 2016), their interaction with inorganic salts would plausibly influence their volatility.

95 In this study, HULIS were extracted from $\text{PM}_{2.5}$ filter samples collected at the SORPES station (Station
96 for observing Regional Processes of the Earth System) in western Yangtze River delta (YRD) during
97 the winter of 2014 to 2015. A Volatility-Hygroscopicity Tandem Differential Mobility Analyzer
98 (VHTDMA) was then used to measure the volatility properties of extracted HULIS and their mixtures
99 with ammonium sulfate. A kinetic mass transfer model was deployed to re-build the measured
100 thermograms, and to separate the mixture into three volatility fractions having an extremely low
101 volatility, low volatility and semi-volatility. Our main goals were (1) to characterize the volatility of
102 size-dependent, re-generated HULIS particles and to get insight into the relationship between
103 atmospheric HULIS and ELVOC, and (2) to understand how the interaction between HULIS and
104 inorganic salts affect their volatilities.

105 2. Methods

106 2.1 Sample collection and HULIS extraction

107 The SORPES station is located on the top of a hill in the Xianlin campus of Nanjing University, which
108 is about 20 km east from the downtown Nanjing and can be regarded as a regional background site of
109 Yangtze River delta (YRD) (Ding et al., 2013; Ding et al., 2016). 24-hour $\text{PM}_{2.5}$ samples were collected
110 on quartz filters using a middle-volume $\text{PM}_{2.5}$ sampler during the winter of 2014 to 2015. HULIS were
111 extracted from four aerosol samples for the following volatility measurements.

112 Water-soluble inorganic ions, organic carbon (OC) and elemental carbon (EC) were measured online
113 using a Monitor for Aerosols and Gases in Air (MARGA) and a sunset OC/EC analyzer during the
114 sampling periods. WSOC were extracted from portions of the sampled filters using sonication in



115 ultrapure water with the ratio of 1 mL water per 1 cm² filter. Insoluble materials were removed by
116 filtering the extracts with a 0.45 μm Teflon filter (Millipore, Billerica, MA, USA). A TOC analyzer
117 with a non-dispersive infrared (NDIR) detector (Shimadzu TOC-VCPH, Japan) was used to determine
118 WSOC concentrations. The aerosol water extracts were then acidified to pH = 2 by HCl and loaded
119 onto a SPE cartridge (Oasis HLB, 30 μm, 60 mg / cartridge, Waters, USA) to isolate the HULIS
120 following the procedure described in Lin et al (2010b). Most of the inorganic ions, low-molecular-
121 weight organic acids and sugars were removed, with HULIS retaining on the SPE cartridge. A total 20
122 ml of methanol was then used to elute the HULIS. The eluate was evaporated to dryness under a gentle
123 stream of nitrogen gas. A part of the HULIS eluate was re-dissolved in 1.0 mL water to be quantified
124 with an evaporative light scattering detector (ELSD).

125 2.2. Volatility measurements by VTDMA measurements

126 The evaporation behavior of HULIS and their mixtures with AS was measured using a Volatility
127 Tandem Mobility Analyzer, which is part of a Volatility-Hygroscopicity Tandem Differential Mobility
128 An-alyzer (VH-TDMA) system (Hong et al., 2014). During the measurements, the hygroscopicity
129 mode was deactivated, so that only the volatility mode of this instrument was functioning. Briefly,
130 aerosol particles were generated by atomizing aqueous solutions consisting of HULIS and their
131 mixtures with AS by using an atomizer (TOPAS, ATM 220). Then, a monodisperse aerosol with
132 particle sizes of 30, 60, 100 and 145 nm were selected by a Hauke-type Differential Mobility Analyzer
133 (DMA, Winklmayr et al., 1991). The monodisperse aerosol flow was then heated by a thermodenuder
134 at a certain temperature, after which the number size distribution of the particles remaining was
135 determined by a second DMA and a condensation particle counter (CPC, TSI 3010). The
136 thermodenuder was a 50-cm-long stainless steel tube with an average residence time of around 5 s.

137 The VTDMA measures the shrinkage of the particle diameter after heating particles of some selected
138 initial size at different temperatures. Conventionally, the volume fraction remaining (VFR), i.e. the
139 fraction of aerosol mass left after heating particles of diameter D_p , is used to describe the evaporation
140 quantitatively. $D_p(T_{room})$ is the initial particle diameter at room temperature. $D_p(T)$ is the particle
141 diameter after passing through the thermodenuder at the temperature T .

142 The VFR can be defined as:



$$143 \quad \text{VFR}(D_p) = \frac{D_p^3(T)}{D_p^3(T_{\text{room}})} \quad (1)$$

144 2.3. Kinetic mass transfer model

145 A kinetic mass transfer model (Riipinen et al., 2010) was applied to help interpreting the HULIS
146 evaporation data. The size distribution, chemical composition and physicochemical properties of the re-
147 generated HULIS particles, as well as the residence time of the particles traveling through the
148 thermodenuder, were predefined in the model. As an output, the model provided the particle mass
149 change as a function of the residence time, which can either increase or decrease depending on the
150 particle composition, volatility of compounds and concentrations of surrounding vapors. With the aim
151 to reproduce the observed evaporation pattern of HULIS particles measured by the VTDMA, the model
152 applied an optimization procedure to minimize the difference between the measured and modeled
153 evaporation curves of the HULIS particles.

154 In the model, particles were assumed to consist of compounds that can be grouped into three volatility
155 bins: semi-volatile, low-volatility and extremely low-volatility components. These three “bins” were
156 quantified by assuming that they had fixed volatilities with $p_{\text{sat}}(298 \text{ K}) = [10^{-3} 10^{-6} 10^{-9}]$ Pa. Modeling
157 was performed for each experiment / sample separately, with 4 samples and 4 different initial particle
158 sizes ($D_p = 30, 60, 100$ and 145 nm), leading to 16 different model runs, each providing information on
159 how much semi-volatile, low-volatile and extremely low-volatility matter (X_i) was present in the
160 investigated particles. The initial particle size refers to the particle diameter prior to heating. The values
161 for $p_{\text{sat}}(298 \text{ K})$ and ΔH_{vap} (see Table 1 and text above) were selected by doing a preliminary test model
162 runs. With ΔH_{vap} of around $[40 40 40]$ kJ mol⁻¹ and $p_{\text{sat}}(298 \text{ K})$ of $[10^{-3} 10^{-6} 10^{-9}]$ Pa the model was
163 best able to reproduce the observed evaporation curves of the HULIS aerosol. Such low vaporization
164 enthalpies (referred often as effective vaporization enthalpies) for aerosol mixtures, for example for
165 SOA from α -pinene oxidation, have been reported also in previous studies (Häkkinen et al.,
166 2014; Donahue et al., 2005; Offenberg et al., 2006; Riipinen et al., 2010). The molecular weight and
167 density of HULIS were assumed to be 280 g mol⁻¹ (Kiss et al., 2003; Lin et al., 2012) and 1.55 kg m⁻³
168 (Dinar et al., 2006), respectively.

169 Volatility information, specifically described as the saturation vapor pressure and vaporization enthalpy
170 here, of ammonium sulfate was determined by interpreting the evaporation behavior of laboratory-
171 generated AS particles using the kinetic evaporation model. By setting the saturation vapor pressures



172 and enthalpy of vaporization of AS as fitting parameters, the optimum solution was obtained by
173 minimizing the difference between the measured and model-interpreted thermograms of AS particles.
174 Hence, p_{sat} (298 K) of $1.9 \cdot 10^{-8}$ Pa and ΔH_{vap} of 97 kJ mol^{-1} for AS were determined and used in the
175 following analysis.

176 2.4 AMS measurement for oxygen to carbon ratio

177 The O : C (Oxygen to carbon) ratios of re-generated HULIS particles were measured using a high-
178 resolution time-of-flight aerosol mass spectrometer (HR-ToF-AMS, Aerodyne Research Inc., Billerica,
179 USA). Detailed descriptions of the instrument and data processing can be found in previous
180 publications (DeCarlo et al., 2006; Canagaratna et al., 2007). The HULIS solution was atomized to
181 generate poly-dispersed aerosol particles and introduced into AMS. The AMS was operated in V mode
182 and the data was acquired at 5-min saving intervals. The AMS data were analyzed using standard ToF-
183 AMS data analysis toolkits (SQUIRREL version 1.57H and PIKA version 1.16H in Igor Pro software
184 (version 6.22A, WaveMetrics Inc.). For mass calculations, the default relative ionization efficiency
185 (RIE) values 1.1, 1.2, 1.3 and 1.4 for nitrate, sulfate, chloride and organic were applied, respectively.
186 The RIE for ammonium was 2.6, determined from the ionization efficiency calibration. In elemental
187 analysis, the “Improved- Ambient” method was applied to calculate O:C ratios by considering the
188 CHO^+ ion correction (Canagaratna et al., 2015).

189 3. Results and discussions

190 Figure 1 shows the chemical compositions of the four $\text{PM}_{2.5}$ samples, and the oxygen to carbon ratio
191 (O : C) of the extracted HULIS in related samples. The four samples can be classified into two groups
192 based on their $\text{PM}_{2.5}$ concentrations (the sum of all measured chemical compositions), with one group
193 (samples 1 and 2) having the $\text{PM}_{2.5}$ higher than $110 \mu\text{g}/\text{m}^3$ and the other one (samples 3 and 4) having
194 the $\text{PM}_{2.5}$ lower than $40 \mu\text{g}/\text{m}^3$. The concentrations of inorganic compounds (sulfate, nitrate and
195 ammonium) were significantly higher in samples 1 and 2 than in samples 3 and 4. The HULIS
196 concentrations were also higher in samples 1 and 2 (about $9 \mu\text{g}/\text{m}^3$) than in samples 3 and 4 (about 6
197 $\mu\text{g}/\text{m}^3$). The oxidation states of the HULIS, however, did not show any notable differences, showing
198 very high values for all the four samples (O:C > 0.95), indicating that the HULIS in YRD could be
199 mostly secondarily formed even during the relatively clean days. Such high oxidation states suggest
200 further that the extracted HULIS were very likely highly-oxidized, multifunctional compounds (HOMs)
201 originating from multi-phase oxidation (Graber and Rudich, 2006).



202 3.1 Volatility of atmospheric HULIS

203 The volume fraction remaining (VFR) of the HULIS particles as a function of the heating temperature
204 obtained from VTDMA is illustrated in Fig. 2. An overall low volatility was identified for the HULIS
205 particles, with the VFR higher than 55% for the particles of all 4 sizes at the heating temperature of
206 280 °C and residence time of 5 s. Small differences in the volatility could be observed between the
207 samples of high mass concentrations and low mass concentrations in that the evaporation of HULIS in
208 samples 1 and 2 was in general weaker than that in samples 3 and 4. In addition, all the samples started
209 to evaporate from the very beginning of the heating program (around 20 °C to 25 °C) and the
210 evaporation curves varied smoothly, suggesting that the HULIS particles were mixtures of compounds
211 having wide range of saturation vapor pressures.

212 A kinetic mass transfer model was applied to reproduce the observed evaporation of the HULIS, and to
213 estimate the mass fractions of semi-volatile (SVOC, $p_{\text{sat}}(298\text{K}) = 10^{-3}$ Pa), low-volatility (LVOC, p_{sat}
214 (298K) = 10^{-6} Pa) and extremely low-volatility organic components (ELVOC, $p_{\text{sat}}(298\text{K}) = 10^{-9}$ Pa).
215 As shown in Fig. 3, the model performed reasonably well in simulating the “pure” HULIS particles
216 (example for sample 1). Noting that the HULIS mixtures were represented with only three model
217 compounds of different volatilities, the modeled evaporation curves of the HULIS in all samples
218 showed a relatively good agreement with the measured evaporation curves for all the four particle sizes.
219 The shape of the modeled thermograms is not as smooth as that of the measured ones suggesting lower
220 number of volatilities in simulations compared with in the real samples. The model-simulated
221 distributions of SVOC, LVOC and ELVOC of each HULIS sample gave indication on the volatility of
222 HULIS. As shown in Fig. 4, all the HULIS samples consisted of compounds from all the 3 volatility
223 “bins”, further confirming HULIS to be mixtures of compounds with wide range of volatilities. SVOC
224 was estimated to account for only small proportion (less than 20% of the particle mass) of the HULIS
225 samples, while LVOC and ELVOC dominated these samples (78% - 97% of the particle mass),
226 suggesting an overall low volatility of the extracted HULIS. Given that the heating program has the
227 potential to raise the evaporation of HULIS by decomposing large molecules, the real volatility of
228 atmospheric HULIS could be even lower than obtained here.

229 In spite of their overall low values, the volatilities of the HULIS varied between the different samples.
230 The HULIS extracted from the samples of higher particle mass loadings (samples 1 and 2) had, in
231 general, lower volatilities than those extracted from the samples of lower particle mass concentrations



232 (samples 3 and 4). By taking 30 nm particles as an example, sample 2 had the largest mass fraction of
233 ELVOC, up to 72%, followed by sample 1 (66%) and sample 3 (64%), while sample 4 had the least
234 amount of ELVOC (58%). Correspondingly, the mass fraction of SVOC in 30 nm particles was the
235 highest in sample 4 (9%) and the lowest in sample 2 (6%). Several factors, including the molecular
236 weight, oxidation state and molecular structure of the compounds, as well as their interaction with other
237 compounds, can influence the volatility of HULIS. Although there is not enough information to support
238 the final conclusion, we excluded the oxidation state as a key factor here because its variation did not
239 match the volatility changes of the HULIS samples. As can be seen from Figs.1 and 4, sample 2
240 showed the lowest volatility but the third highest oxidation state of the four samples. Instead of the
241 oxidation state, the interaction between HULIS and inorganic species is a more likely candidate for
242 influencing the observed variation of the HULIS volatility, especially as the lower-volatility samples
243 (sample 1 and sample 2) had higher concentrations and fractions of inorganic species (Fig. 1).

244 Within individual HULIS samples, the estimated amount of ELVOC, LVOC and SVOC varied with the
245 particle size (Fig. 4). The mass fraction of ELVOC was in the range of 58–72% for the smallest
246 particles (30 nm in diameter) and decreased to the range of 47–60% for the 60 nm, to the range of
247 35–53% for the 100 nm particles, and to the range of 20–39% for the 145 nm particles. The amount of
248 LVOC increased correspondingly with an increasing particle size, from 23–33% for the 30 nm particles
249 to 52–65% for the 145 nm particles. The amount of SVOC slightly increased with an increasing
250 particle size, on average from 7.5% (30 nm) to 14.5% (145 nm). The most likely explanation for this
251 behavior is that, due to the Kelvin effect, compounds with higher volatilities are likely to evaporate
252 more from smaller particles. This result indicates that size-resolved chemical compositions of
253 laboratory-generated particles from aqueous solutions of mixtures should be examined more carefully
254 to support their size-dependent physical properties from lab studies.

255 3.2 Interaction between HULIS and ammonium sulfate

256 Interactions between inorganic and organic matter have been shown to influence the volatility of the
257 organic matter. However, recent work has focused on the interaction between one specific organic
258 compound and some inorganic salt(s). For example, Laskin et al. (2012) observed the formation of
259 sodium organic salt in a submicron organic acid-NaCl aerosol. Ma et al. (2013) reported that the
260 formation of sodium oxalate can occur in particles containing oxalic acid and sodium chloride.
261 Häkkinen et al. (2014) demonstrated that low-volatility material, such as organic salts, were formed



262 within aerosol mixtures of inorganic compounds with organic acids. Zardini et al. (2010) and Yli-Juuti
263 et al. (2013b) suggested that interactions between inorganic salts and organic acids in the particle phase
264 might further enhance the partitioning of organic acids onto the particle phase. Given the complex
265 nature of organic aerosols in the real atmosphere, large uncertainties will be induced when using
266 simplified laboratory results for explaining observations in the real atmosphere. In this study, we
267 investigated the volatility of mixed samples of HULIS and ammonium sulfate in different ratios in
268 order to get better understand organic-inorganic interactions under atmospherically relevant conditions.

269 Three samples were prepared by mixing HULIS (extracted from sample 1) and pure ammonium sulfate
270 (AS) with the mass ratios (HULIS to AS) of 0.25:0.75, 0.5:0.5 and 0.75:0.25 (actually 0.29:0.71,
271 0.55:0.45 and 0.79:0.21). As shown by Fig. 5, pure ammonium sulfate particles started to evaporate at
272 100°C, and were almost entirely evaporated at 180 °C, whereas HULIS aerosol started to evaporate at
273 the very beginning (about 20 °C) and more than 80% of its volume still remained at 180 °C. The
274 evaporation curves for the three mixed samples (Fig. 6) showed generally slow evaporation rates within
275 the temperature windows from 20 °C to 100 °C and from 180 °C to 280 °C, and much faster
276 evaporation rates between 100 °C and 180 °C. Interactions between HULIS and ammonium sulfate
277 obviously influenced the observed volatility. For example, the VFRs of 0.25:0.75 samples (Fig. 6a) at
278 the temperature of 180 °C were around 0.4 (varied from 0.397 to 0.428 for different size particles),
279 which is significantly higher than the calculated VFR ($0.29 \times 0.8 + 0.71 \times 0.06 = 0.275$) by assuming
280 HULIS and ammonium sulfate independently separated. This indicates that mixing of ammonium
281 sulfate to a HULIS solution decreases the volatility of the organic group or, alternatively, forms new
282 compounds of low volatility. For the 0.5:0.5 and 0.75:0.25 samples (Fig. 6b and 6c), the VFRs at
283 180 °C were around 0.43 (0.395 to 0.460 for different size particles) and 0.64 (0.595 to 0.655), which
284 are comparable to the calculated VFR (0.467 for the 0.5:0.5 samples and 0.645 for the 0.75:0.25
285 samples). These results indicate that the role of HULIS-AS interactions in the volatility of their
286 mixtures is complex and nonlinear.

287 In order to quantify the volatility changes of HULIS induced by its interaction with ammonium sulfate,
288 the kinetic mass transfer model was again applied to estimate the mass fractions of SVOC, LVOC and
289 ELVOC for the HULIS part in the mixed samples. As shown in Fig. 7, the model's performance in
290 simulating mixed HULIS-AS samples was fairly good, yet poorer than in simulating the "pure" HULIS
291 sample. The poorest agreement between the simulated and measured evaporation curves was found for



292 the 1:3 mixed samples (mass ratio of HULIS to AS), indicating relatively high uncertainties in the
293 calculated mass fractions of compounds with different volatility bins for this mixture. These visible
294 differences between modeled and measured results indicate that interactions between HULIS and AS
295 indeed influence their volatility distribution. As can be seen from Fig. 8, the estimated fraction of
296 ELVOC in the HULIS part of the 0:25:0.75 (Fig. 8b) and 0.75:0.25 (Fig. 8d) samples was much higher
297 than in the pure HULIS sample (Fig. 8a), while the ELVOC fraction in the 0.5:0.5 sample was
298 comparable to that in the pure HULIS sample. By taking 30 nm and 145 nm particles as an example,
299 the corresponding estimated ELVOC fractions were 0.66 and 0.26 in the pure HULIS sample, 1.0 and
300 0.93 in the 0.25:0.75 sample, 0.53 and 0.45 in the 0.5:0.5 sample, and 0.83 and 0.71 in the 0.75:0.25
301 sample, respectively. In spite of the possible overestimation of ELVOCs fraction in 1:3 mixed samples,
302 these results suggest that the interaction between HULIS and ammonium sulfate tend to decrease the
303 volatility of HULIS, and that this effect is nonlinear.

304 4. Conclusion and implication

305 In this study, we analyzed the volatility of atmospheric HULIS extracted from four PM_{2.5} samples
306 collected at the SORPES station in the western YRD of eastern China, and investigated how the
307 interactions between HULIS and ammonium sulfate affected the volatility of HULIS aerosol fraction.
308 Overall, low volatilities and high oxidation states were identified for all the four samples, with VFRs at
309 280°C being higher than 55 % and O to C ratio being higher than 0.95 for all the re-generated HULIS
310 particles. A kinetic mass transfer model was deployed to divide the HULIS mixture into SVOC, LVOC
311 and ELVOC groups. We found that HULIS were dominated by LVOC and ELVOC (more than 80%)
312 compounds. Given the possible thermo-decomposition of large molecules during the heating program,
313 an even lower volatility than found here is possible for atmospheric HULIS in eastern China. The
314 Kelvin effect was supposedly taking place in atomizing the solutions of the HULIS mixtures, which
315 resulted in a size dependent distribution of the relative fractions of SVOC, LVOC and ELVOC in the
316 generated particles. The interaction between HULIS and ammonium sulfate was found to decrease the
317 volatility of the HULIS part in the mixed samples. However, these volatility changes were not linearly
318 correlated with the mass fractions of ammonium sulfate, indicating a complex interaction between the
319 HULIS mixture and inorganic salts.

320 This study demonstrates that HULIS are important low volatility and extremely low volatility
321 compounds in the aerosol phase, and sheds new light on the connection between atmospheric HULIS



322 and ELVOCs. In a view of the important sources of HULIS, multi-phase processes, including multi-
323 phase oxidation, oligomerization, polymerization and interaction with inorganic salts, have the
324 potential to lower the volatility of organic compounds in the aerosol phase, and to influence their gas-
325 aerosol partitioning. Multiphase processes could be one of the important reasons that most models tend
326 to underestimate the formation of SOA.

327 **Acknowledgements**

328 This work was funded by National Natural Science Foundation of China (D0512/41675145 and D0510/
329 41505109), and the National Key Research Program (2016YFC0202002 and 2016YFC0200506).

330 **References:**

- 331 Aiken, A. C., DeCarlo, P. F., Kroll, J. H., Worsnop, D. R., Huffman, J. A., Docherty, K. S., Ulbrich, I. M., Mohr,
332 C., Kimmel, J. R., Sueper, D., Sun, Y., Zhang, Q., Trimborn, A., Northway, M., Ziemann, P. J., Canagaratna, M.
333 R., Onasch, T. B., Alfarra, M. R., Prevot, A. S. H., Dommen, J., Duplissy, J., Metzger, A., Baltensperger, U., and
334 Jimenez, J. L.: O/C and OM/OC Ratios of Primary, Secondary, and Ambient Organic Aerosols with High-
335 Resolution Time-of-Flight Aerosol Mass Spectrometry, *Environ. Sci. Technol.*, 42, 4478-4485,
336 10.1021/es703009q, 2008.
- 337 Bilde, M., Barsanti, K., Booth, M., Cappa, C. D., Donahue, N. M., Emanuelsson, E. U., McFiggans, G., Krieger,
338 U. K., Marcolli, C., Topping, D., Ziemann, P., Barley, M., Clegg, S., Dennis-Smith, B., Hallquist, M.,
339 Hallquist, Å. M., Khlystov, A., Kulmala, M., Mogensen, D., Percival, C. J., Pope, F., Reid, J. P., Ribeiro da
340 Silva, M. A. V., Rosenoern, T., Salo, K., Soonsin, V. P., Yli-Juuti, T., Prisle, N. L., Pagels, J., Rarey, J., Zardini,
341 A. A., and Riipinen, I.: Saturation Vapor Pressures and Transition Enthalpies of Low-Volatility Organic
342 Molecules of Atmospheric Relevance: From Dicarboxylic Acids to Complex Mixtures, *Chem. Rev.*, 115, 4115-
343 4156, 10.1021/cr5005502, 2015.
- 344 Canagaratna, M. R., Jayne, J. T., Jimenez, J. L., Allan, J. D., Alfarra, M. R., Zhang, Q., Onasch, T. B., Drewnick,
345 F., Coe, H., Middlebrook, A., Delia, A., Williams, L. R., Trimborn, A. M., Northway, M. J., DeCarlo, P. F.,
346 Kolb, C. E., Davidovits, P., and Worsnop, D. R.: Chemical and microphysical characterization of ambient
347 aerosols with the aerodyne aerosol mass spectrometer, *Mass Spectrom. Rev.*, 26, 185-222, 10.1002/mas.20115,
348 2007.
- 349 Canagaratna, M. R., Jimenez, J. L., Kroll, J. H., Chen, Q., Kessler, S. H., Massoli, P., Hildebrandt Ruiz, L.,
350 Fortner, E., Williams, L. R., Wilson, K. R., Surratt, J. D., Donahue, N. M., Jayne, J. T., and Worsnop, D. R.:



- 351 Elemental ratio measurements of organic compounds using aerosol mass spectrometry: characterization,
352 improved calibration, and implications, *Atmos. Chem. Phys.*, 15, 253-272, 10.5194/acp-15-253-2015, 2015.
- 353 Chen, Q., Ikemori, F., Higo, H., Asakawa, D., and Mochida, M.: Chemical Structural Characteristics of HULIS
354 and Other Fractionated Organic Matter in Urban Aerosols: Results from Mass Spectral and FT-IR Analysis,
355 *Environ. Sci. Technol.*, 50, 1721-1730, 10.1021/acs.est.5b05277, 2016.
- 356 DeCarlo, P. F., Kimmel, J. R., Trimborn, A., Northway, M. J., Jayne, J. T., Aiken, A. C., Gonin, M., Fuhrer, K.,
357 Horvath, T., Docherty, K. S., Worsnop, D. R., and Jimenez, J. L.: Field-Deployable, High-Resolution, Time-of-
358 Flight Aerosol Mass Spectrometer, *Anal. Chem.*, 78, 8281-8289, 10.1021/ac061249n, 2006.
- 359 Dinar, E., Mentel, T. F., and Rudich, Y.: The density of humic acids and humic like substances (HULIS) from
360 fresh and aged wood burning and pollution aerosol particles, *Atmos. Chem. Phys.*, 6, 5213-5224, 10.5194/acp-6-
361 5213-2006, 2006.
- 362 Ding, A. J., Fu, C. B., Yang, X. Q., Sun, J. N., Zheng, L. F., Xie, Y. N., Herrmann, E., Nie, W., Petäjä, T.,
363 Kerminen, V. M., and Kulmala, M.: Ozone and fine particle in the western Yangtze River Delta: an overview of
364 1 yr data at the SORPES station, *Atmos. Chem. Phys.*, 13, 5813-5830, 10.5194/acp-13-5813-2013, 2013.
- 365 Ding, A. J., Nie, W., Huang, X., Chi, X., Sun, J., Kerminen, V. M., Xu, Z., Guo, W., Petaja, T., Yang, X. Q.,
366 Kulmala, M., and Fu, C.: Long-term observation of air pollution-weather/climate interactions at the SORPES
367 station: A review and outlook, *Front. Environ. Sci. Eng.*, 2016.
- 368 Donahue, N. M., Hartz, K. E. H., Chuong, B., Presto, A. A., Stanier, C. O., Rosenhørn, T., Robinson, A. L., and
369 Pandis, S. N.: Critical factors determining the variation in SOA yields from terpene ozonolysis: A combined
370 experimental and computational study, *Faraday Discuss.*, 130, 295-309, 2005.
- 371 Donahue, N. M., Kroll, J. H., Pandis, S. N., and Robinson, A. L.: A two-dimensional volatility basis set – Part 2:
372 Diagnostics of organic-aerosol evolution, *Atmos. Chem. Phys.*, 12, 615-634, 10.5194/acp-12-615-2012, 2012.
- 373 Ehn, M., Thornton, J. A., Kleist, E., Sipila, M., Junninen, H., Pullinen, I., Springer, M., Rubach, F., Tillmann, R.,
374 Lee, B., Lopez-Hilfiker, F., Andres, S., Acir, I.-H., Rissanen, M., Jokinen, T., Schobesberger, S., Kangasluoma,
375 J., Kontkanen, J., Nieminen, T., Kurten, T., Nielsen, L. B., Jorgensen, S., Kjaergaard, H. G., Canagaratna, M.,
376 Maso, M. D., Berndt, T., Petaja, T., Wahner, A., Kerminen, V.-M., Kulmala, M., Worsnop, D. R., Wildt, J., and
377 Mentel, T. F.: A large source of low-volatility secondary organic aerosol, *Nature*, 506, 476-479,
378 10.1038/nature13032, 2014.
- 379 Graber, E. R., and Rudich, Y.: Atmospheric HULIS: How humic-like are they? A comprehensive and critical
380 review, *Atmos. Chem. Phys.*, 6, 729-753, 10.5194/acp-6-729-2006, 2006.



- 381 Häkkinen, S. A. K., McNeill, V. F., and Riipinen, I.: Effect of Inorganic Salts on the Volatility of Organic Acids,
382 Environ. Sci. Technol., 48, 13718-13726, 10.1021/es5033103, 2014.
- 383 Hoffer, A., Gelencsér, A., Guyon, P., Kiss, G., Schmid, O., Frank, G. P., Artaxo, P., and Andreae, M. O.: Optical
384 properties of humic-like substances (HULIS) in biomass-burning aerosols, Atmos. Chem. Phys., 6, 3563-3570,
385 10.5194/acp-6-3563-2006, 2006.
- 386 Hong, J., Häkkinen, S. A. K., Paramonov, M., Äijälä, M., Hakala, J., Nieminen, T., Mikkilä, J., Prisle, N. L.,
387 Kulmala, M., Riipinen, I., Bilde, M., Kerminen, V. M., and Petäjä, T.: Hygroscopicity, CCN and volatility
388 properties of submicron atmospheric aerosol in a boreal forest environment during the summer of 2010, Atmos.
389 Chem. Phys., 14, 4733-4748, 10.5194/acp-14-4733-2014, 2014.
- 390 Jimenez, J. L., Canagaratna, M. R., Donahue, N. M., Prevot, A. S. H., Zhang, Q., Kroll, J. H., DeCarlo, P. F.,
391 Allan, J. D., Coe, H., Ng, N. L., Aiken, A. C., Docherty, K. S., Ulbrich, I. M., Grieshop, A. P., Robinson, A. L.,
392 Duplissy, J., Smith, J. D., Wilson, K. R., Lanz, V. A., Hueglin, C., Sun, Y. L., Tian, J., Laaksonen, A.,
393 Raatikainen, T., Rautiainen, J., Vaattovaara, P., Ehn, M., Kulmala, M., Tomlinson, J. M., Collins, D. R., Cubison,
394 M. J., E., Dunlea, J., Huffman, J. A., Onasch, T. B., Alfarra, M. R., Williams, P. I., Bower, K., Kondo, Y.,
395 Schneider, J., Drewnick, F., Borrmann, S., Weimer, S., Demerjian, K., Salcedo, D., Cottrell, L., Griffin, R.,
396 Takami, A., Miyoshi, T., Hatakeyama, S., Shimono, A., Sun, J. Y., Zhang, Y. M., Dzepina, K., Kimmel, J. R.,
397 Sueper, D., Jayne, J. T., Herndon, S. C., Trimborn, A. M., Williams, L. R., Wood, E. C., Middlebrook, A. M.,
398 Kolb, C. E., Baltensperger, U., and Worsnop, D. R.: Evolution of Organic Aerosols in the Atmosphere, Science,
399 326, 1525-1529, 10.1126/science.1180353, 2009.
- 400 Kanakidou, M., Seinfeld, J. H., Pandis, S. N., Barnes, I., Dentener, F. J., Facchini, M. C., Van Dingenen, R.,
401 Ervens, B., Nenes, A., Nielsen, C. J., Swietlicki, E., Putaud, J. P., Balkanski, Y., Fuzzi, S., Horth, J., Moortgat,
402 G. K., Winterhalter, R., Myhre, C. E. L., Tsigaridis, K., Vignati, E., Stephanou, E. G., and Wilson, J.: Organic
403 aerosol and global climate modelling: a review, Atmos. Chem. Phys., 5, 1053-1123, 10.5194/acp-5-1053-2005,
404 2005.
- 405 Kiss, G., Tombác, E., Varga, B., Alsberg, T., and Persson, L.: Estimation of the average molecular weight of
406 humic-like substances isolated from fine atmospheric aerosol, Atmos. Environ., 37, 3783-3794,
407 [http://dx.doi.org/10.1016/S1352-2310\(03\)00468-0](http://dx.doi.org/10.1016/S1352-2310(03)00468-0), 2003.
- 408 Kiss, G., Tombác, E., and Hansson, H.-C.: Surface Tension Effects of Humic-Like Substances in the Aqueous
409 Extract of Tropospheric Fine Aerosol, J. Atmos. Chem., 50, 279-294, 10.1007/s10874-005-5079-5, 2005.
- 410 Kristensen, T. B., Wex, H., Nekat, B., Nøjgaard, J. K., van Pinxteren, D., Lowenthal, D. H., Mazzoleni, L. R.,
411 Dieckmann, K., Bender Koch, C., Mentel, T. F., Herrmann, H., Gannet Hallar, A., Stratmann, F., and Bilde, M.:



- 412 Hygroscopic growth and CCN activity of HULIS from different environments, *J. Geophys. Res.-Atmos.*, 117,
413 n/a-n/a, 10.1029/2012JD018249, 2012.
- 414 Kristensen, T. B., Prisle, N. L., and Bilde, M.: Cloud droplet activation of mixed model HULIS and NaCl
415 particles: Experimental results and κ -Köhler theory, *Atmos. Res.*, 137, 167-175,
416 <http://dx.doi.org/10.1016/j.atmosres.2013.09.017>, 2014.
- 417 Kristensen, T. B., Du, L., Nguyen, Q. T., Nøjgaard, J. K., Koch, C. B., Nielsen, O. F., Hallar, A. G., Lowenthal,
418 D. H., Nekat, B., Pinxteren, D. v., Herrmann, H., Glasius, M., Kjaergaard, H. G., and Bilde, M.: Chemical
419 properties of HULIS from three different environments, *J. Atmos. Chem.*, 72, 65-80, 10.1007/s10874-015-9302-
420 8, 2015.
- 421 Krivácsy, Z., Kiss, G., Ceburnis, D., Jennings, G., Maenhaut, W., Salma, I., and Shooter, D.: Study of water-
422 soluble atmospheric humic matter in urban and marine environments, *Atmos. Res.*, 87, 1-12,
423 <http://dx.doi.org/10.1016/j.atmosres.2007.04.005>, 2008.
- 424 Kroll, J. H., and Seinfeld, J. H.: Chemistry of secondary organic aerosol: Formation and evolution of low-
425 volatility organics in the atmosphere, *Atmos. Environ.*, 42, 3593-3624,
426 <http://dx.doi.org/10.1016/j.atmosenv.2008.01.003>, 2008.
- 427 Laskin, A., Moffet, R. C., Gilles, M. K., Fast, J. D., Zaveri, R. A., Wang, B., Nigge, P., and Shutthanandan, J.:
428 Tropospheric chemistry of internally mixed sea salt and organic particles: Surprising reactivity of NaCl with
429 weak organic acids, *J. Geophys. Res.-Atmos.*, 117, D15302, 10.1029/2012jd017743, 2012.
- 430 Lin, P., Engling, G., and Yu, J. Z.: Humic-like substances in fresh emissions of rice straw burning and in
431 ambient aerosols in the Pearl River Delta Region, China, *Atmos. Chem. Phys.*, 10, 6487-6500, 10.5194/acp-10-
432 6487-2010, 2010a.
- 433 Lin, P., Huang, X.-F., He, L.-Y., and Zhen Yu, J.: Abundance and size distribution of HULIS in ambient
434 aerosols at a rural site in South China, *J. Aerosol Sci.*, 41, 74-87,
435 <http://dx.doi.org/10.1016/j.jaerosci.2009.09.001>, 2010b.
- 436 Lin, P., and Yu, J. Z.: Generation of Reactive Oxygen Species Mediated by Humic-like Substances in
437 Atmospheric Aerosols, *Environ. Sci. Technol.*, 45, 10362-10368, 10.1021/es2028229, 2011.
- 438 Lin, P., Rincon, A. G., Kalberer, M., and Yu, J. Z.: Elemental Composition of HULIS in the Pearl River Delta
439 Region, China: Results Inferred from Positive and Negative Electrospray High Resolution Mass Spectrometric
440 Data, *Environ. Sci. Technol.*, 46, 7454-7462, 10.1021/es300285d, 2012.
- 441 Lukács, H., Gelencsér, A., Hammer, S., Puxbaum, H., Pio, C., Legrand, M., Kasper-Giebl, A., Handler, M.,
442 Limbeck, A., Simpson, D., and Preunkert, S.: Seasonal trends and possible sources of brown carbon based on 2-



- 443 year aerosol measurements at six sites in Europe, *J. Geophys. Res.-Atmos.*, 112, n/a-n/a, 10.1029/2006JD008151,
444 2007.
- 445 Ma, Q., Ma, J., Liu, C., Lai, C., and He, H.: Laboratory Study on the Hygroscopic Behavior of External and
446 Internal C₂-C₄ Dicarboxylic Acid-NaCl Mixtures, *Environ. Sci. Technol.*, 47, 10381-10388,
447 10.1021/es4023267, 2013.
- 448 Murphy, B. N., Donahue, N. M., Robinson, A. L., and Pandis, S. N.: A naming convention for atmospheric
449 organic aerosol, *Atmos. Chem. Phys.*, 14, 5825-5839, 10.5194/acp-14-5825-2014, 2014.
- 450 Offenberg, J. H., Kleindienst, T. E., Jaoui, M., Lewandowski, M., and Edney, E. O.: Thermal properties of
451 secondary organic aerosols, *Geophys. Res. Lett.*, 33, n/a-n/a, 10.1029/2005GL024623, 2006.
- 452 Ortiz-Montalvo, D. L., Häkkinen, S. A. K., Schwier, A. N., Lim, Y. B., McNeill, V. F., and Turpin, B. J.:
453 Ammonium addition (and aerosol pH) has a dramatic impact on the volatility and yield of glyoxal secondary
454 organic aerosol, *Environ. Sci. Technol.*, 48, 255-262, 10.1021/es4035667, 2014.
- 455 Paciga, A. L., Riipinen, I., and Pandis, S. N.: Effect of ammonia on the volatility of organic diacids, *Environ. Sci.*
456 *Technol.*, 48, 13769-13775, 10.1021/es5037805, 2014.
- 457 Paglione, M., Kiendler-Scharr, A., Mensah, A. A., Finessi, E., Giulianelli, L., Sandrini, S., Facchini, M. C.,
458 Fuzzi, S., Schlag, P., Piazzalunga, A., Tagliavini, E., Henzing, J. S., and Decesari, S.: Identification of humic-
459 like substances (HULIS) in oxygenated organic aerosols using NMR and AMS factor analyses and liquid
460 chromatographic techniques, *Atmos. Chem. Phys.*, 14, 25-45, 10.5194/acp-14-25-2014, 2014.
- 461 Riipinen, I., Pierce, J. R., Donahue, N. M., and Pandis, S. N.: Equilibration time scales of organic aerosol inside
462 thermodenuders: Evaporation kinetics versus thermodynamics, *Atmos. Environ.*, 44, 597-607,
463 <http://dx.doi.org/10.1016/j.atmosenv.2009.11.022>, 2010.
- 464 Verma, V., Rico-Martinez, R., Kotra, N., King, L., Liu, J., Snell, T. W., and Weber, R. J.: Contribution of
465 Water-Soluble and Insoluble Components and Their Hydrophobic/Hydrophilic Subfractions to the Reactive
466 Oxygen Species-Generating Potential of Fine Ambient Aerosols, *Environ. Sci. Technol.*, 46, 11384-11392,
467 10.1021/es302484r, 2012.
- 468 Wex, H., Hennig, T., Salma, I., Ocskay, R., Kiselev, A., Henning, S., Massling, A., Wiedensohler, A., and
469 Stratmann, F.: Hygroscopic growth and measured and modeled critical super-saturations of an atmospheric
470 HULIS sample, *Geophys. Res. Lett.*, 34, n/a-n/a, 10.1029/2006GL028260, 2007.
- 471 Winklmayr, W., Reischl, G. P., Lindner, A. O., and Berner, A.: A new electromobility spectrometer for the
472 measurement of aerosol size distributions in the size range from 1 to 1000 nm, *J. Aerosol Sci.*, 22, 289-296,
473 [http://dx.doi.org/10.1016/S0021-8502\(05\)80007-2](http://dx.doi.org/10.1016/S0021-8502(05)80007-2), 1991.



- 474 Yli-Juuti, T., Zardini, A. A., Eriksson, A. C., Hansen, A. M., Pagels, J. H., Swietlicki, E., Svenningsson, B.,
475 Glasius, M., Worsnop, D. R., Riipinen, I., and Bilde, M.: Volatility of organic aerosol: Evaporation of
476 ammonium sulfate/succinic acid aqueous solution droplets, *Environ. Sci. Technol.*, 47, 12123-12130,
477 10.1021/es401233c, 2013.
- 478 Zardini, A. A., Riipinen, I., Koponen, I. K., Kulmala, M., and Bilde, M.: Evaporation of ternary
479 inorganic/organic aqueous droplets: Sodium chloride, succinic acid and water, *J. Aerosol Sci.*, 41, 760-770,
480 10.1016/j.jaerosci.2010.05.003, 2010.
- 481 Zhang, Q., Jimenez, J. L., Canagaratna, M. R., Allan, J. D., Coe, H., Ulbrich, I., Alfarra, M. R., Takami, A.,
482 Middlebrook, A. M., Sun, Y. L., Dzepina, K., Dunlea, E., Docherty, K., DeCarlo, P. F., Salcedo, D., Onasch, T.,
483 Jayne, J. T., Miyoshi, T., Shimojo, A., Hatakeyama, S., Takegawa, N., Kondo, Y., Schneider, J., Drewnick, F.,
484 Borrmann, S., Weimer, S., Demerjian, K., Williams, P., Bower, K., Bahreini, R., Cottrell, L., Griffin, R. J.,
485 Rautiainen, J., Sun, J. Y., Zhang, Y. M., and Worsnop, D. R.: Ubiquity and dominance of oxygenated species in
486 organic aerosols in anthropogenically-influenced Northern Hemisphere midlatitudes, *Geophys. Res. Lett.*, 34,
487 n/a-n/a, 10.1029/2007GL029979, 2007.



Table 1 Kinetic model input settings for three-component HULIS aerosol.

Model input parameter	Unit	HULIS
Molar mass, M	g mol^{-1}	[280 280 280]
Density, ρ	kg m^{-3}	[1550 1550 1550]
Surface tension, σ	N m^{-1}	[0.05 0.05 0.05]
Diffusion coefficient, D	$10^{-6} \text{ m}^2 \text{ s}^{-1}$	[5 5 5]
Parameter for the calculation of T -dependence of D , μ	-	[1.75 1.75 1.75]
Saturation vapor pressure, p_{sat} (298 K)	Pa	[10^{-3} 10^{-6} 10^{-9}]
Saturation vapor concentration, c_{sat} (298 K)	$\mu\text{g m}^{-3}$	[10^2 10^{-1} 10^{-4}]
Enthalpy of vaporization, ΔH_{vap}	kJ mol^{-1}	[40 40 40]
Mass accommodation coefficient, α_{m}	-	[1 1 1]
Activity coefficient, γ	-	[1 1 1]
Particle initial diameter, d_{p}	nm	30, 60, 100, 145
Particle total mass, $m_{\text{p,tot}}$	$\mu\text{g m}^{-3}$	1
		Thermodenuder
Length of the flow tube	m	0.50 (i.d of 6 mm)
Residence time	s	5

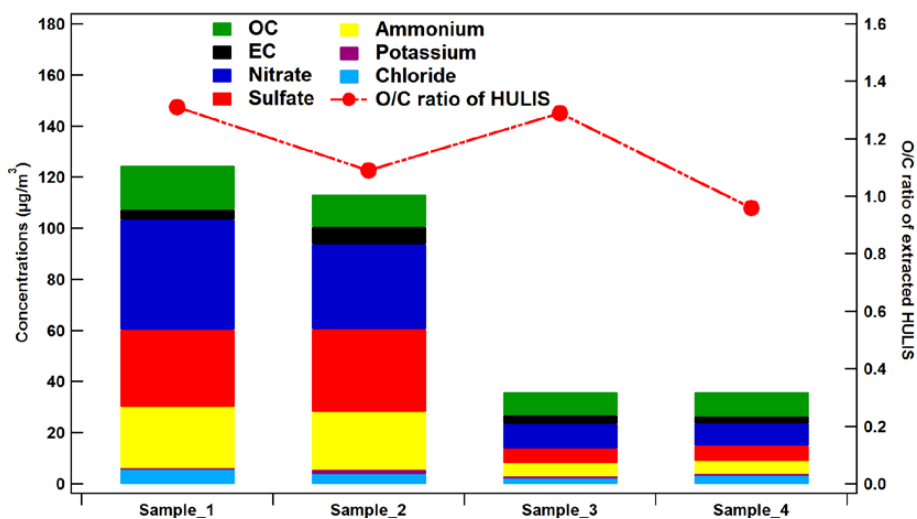


Figure 1 Chemical composition of the four PM_{2.5} samples collected at SORPES station and oxygen to carbon ratio of extracted HULIS from related samples

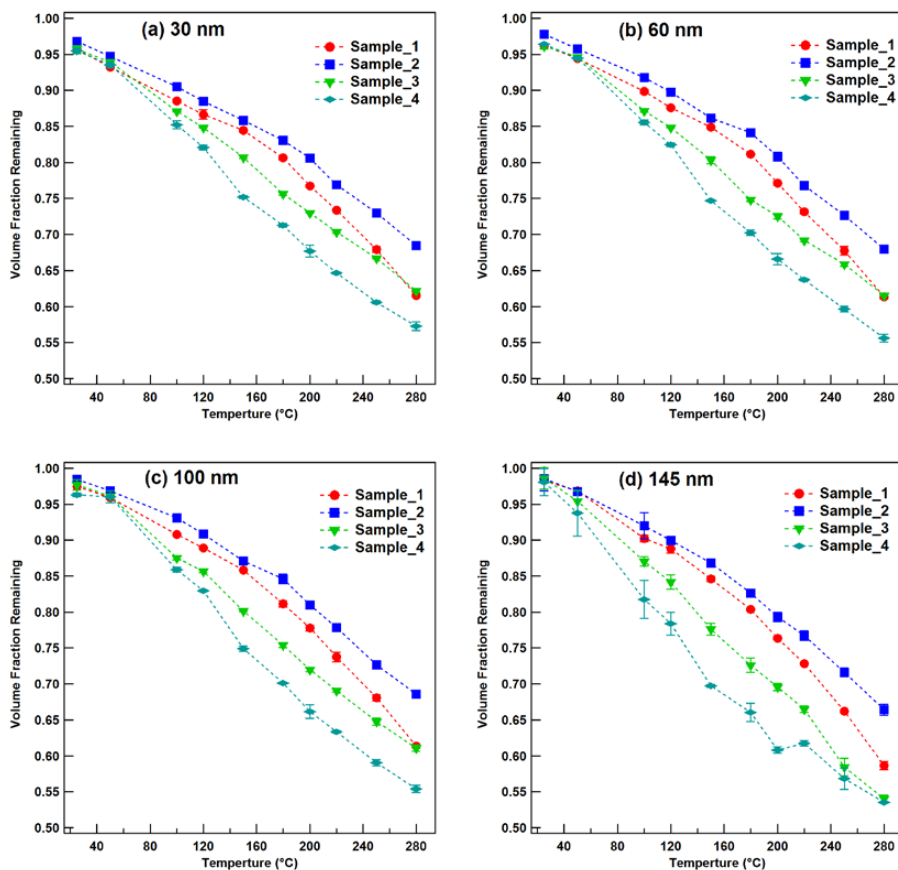


Figure 2 Volume fraction remaining (VFR) as a function of heating temperature for 4 samples at four different sizes of (a) 30 nm, (b) 60 nm, (c) 100 nm, and (d) 145 nm

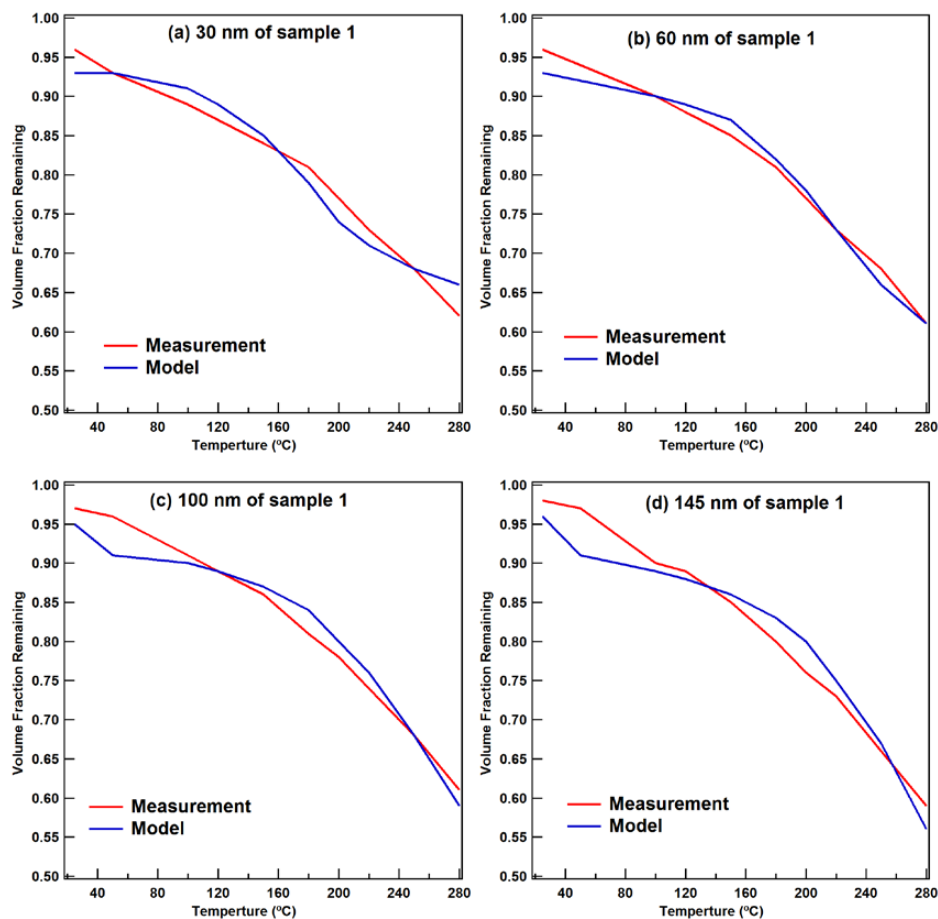


Figure 3 Measured and modeled volume fraction remaining (VFR) as a function of temperature for HULIS of sample 1 at four different particle sizes of (a) 30 nm, (b) 60 nm, (c) 100 nm and (d) 145 nm

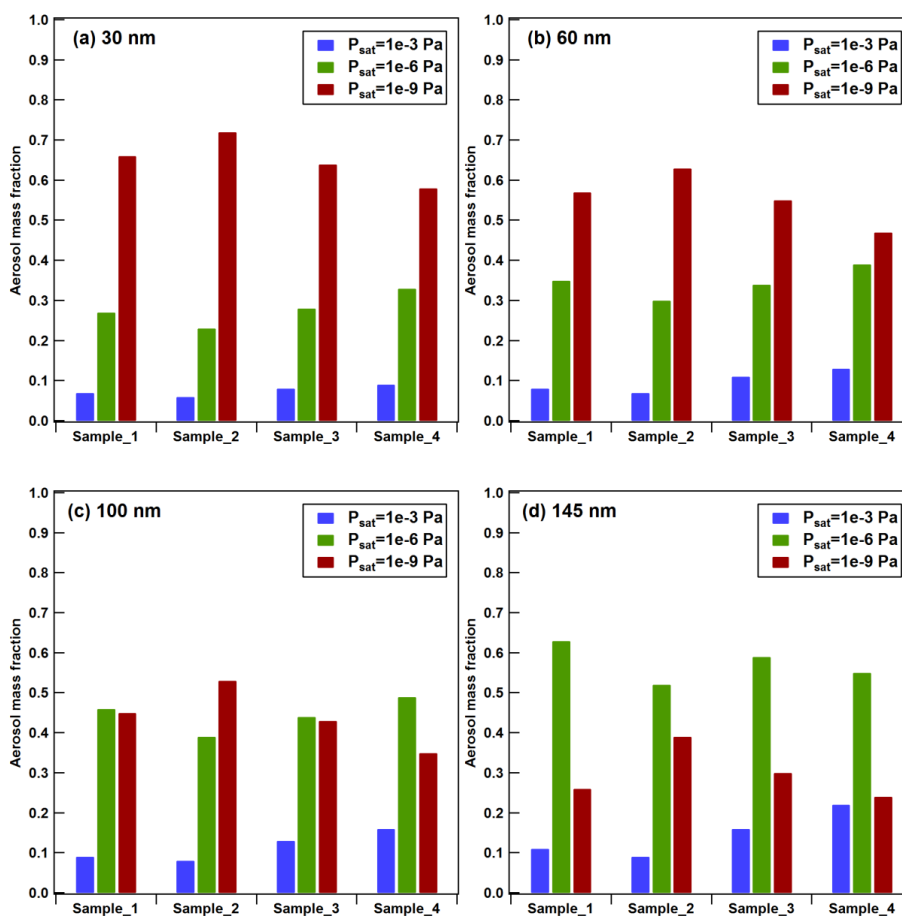


Figure 4 Mass fractions of compounds of SVOC ($p_{\text{sat}}=10^{-3}$ Pa), LVO ($p_{\text{sat}}=10^{-6}$ Pa) and ELVOC, ($p_{\text{sat}}=10^{-9}$ Pa) in four aerosol samples with different particle sizes of (a) 30 nm, (b) 60 nm, (c) 100 nm, and (d) 145 nm

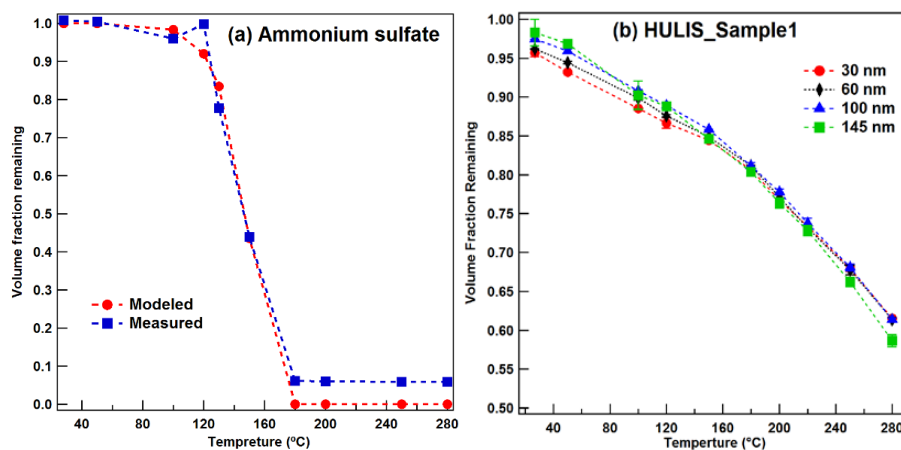


Figure 5 Volume fraction remaining (VFR) as a function of heating temperature for (a) measured and modeled pure ammonium sulfate particles at 100 nm, and (b) HULIS sample 1 at four different sizes of 30 nm, 60 nm, 100 nm, and 145 nm

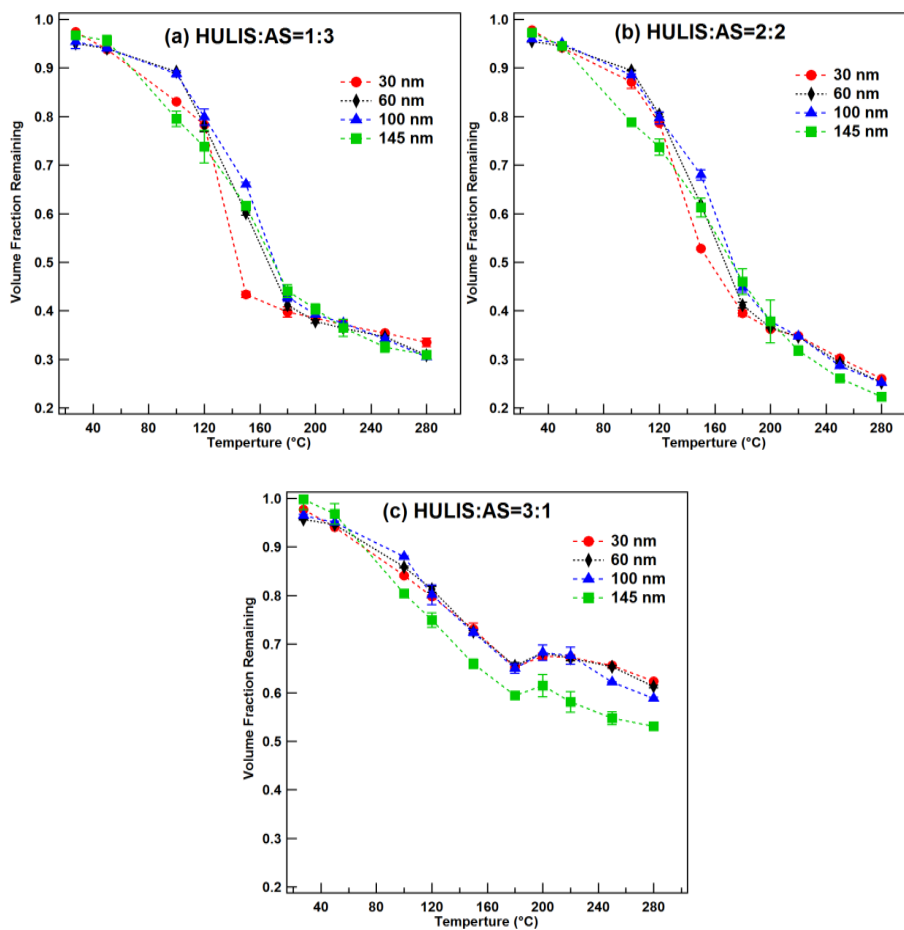


Figure 6 Volume fraction remaining (VFR) as a function of heating temperature for (a) 1:3 HULIS-AS mixed sample, (b) 2:2 HULIS-AS mixed samples, and (c) 3:1 HULIS-AS mixed samples at four different sizes of 30 nm, 60 nm, 100 nm, and 145 nm

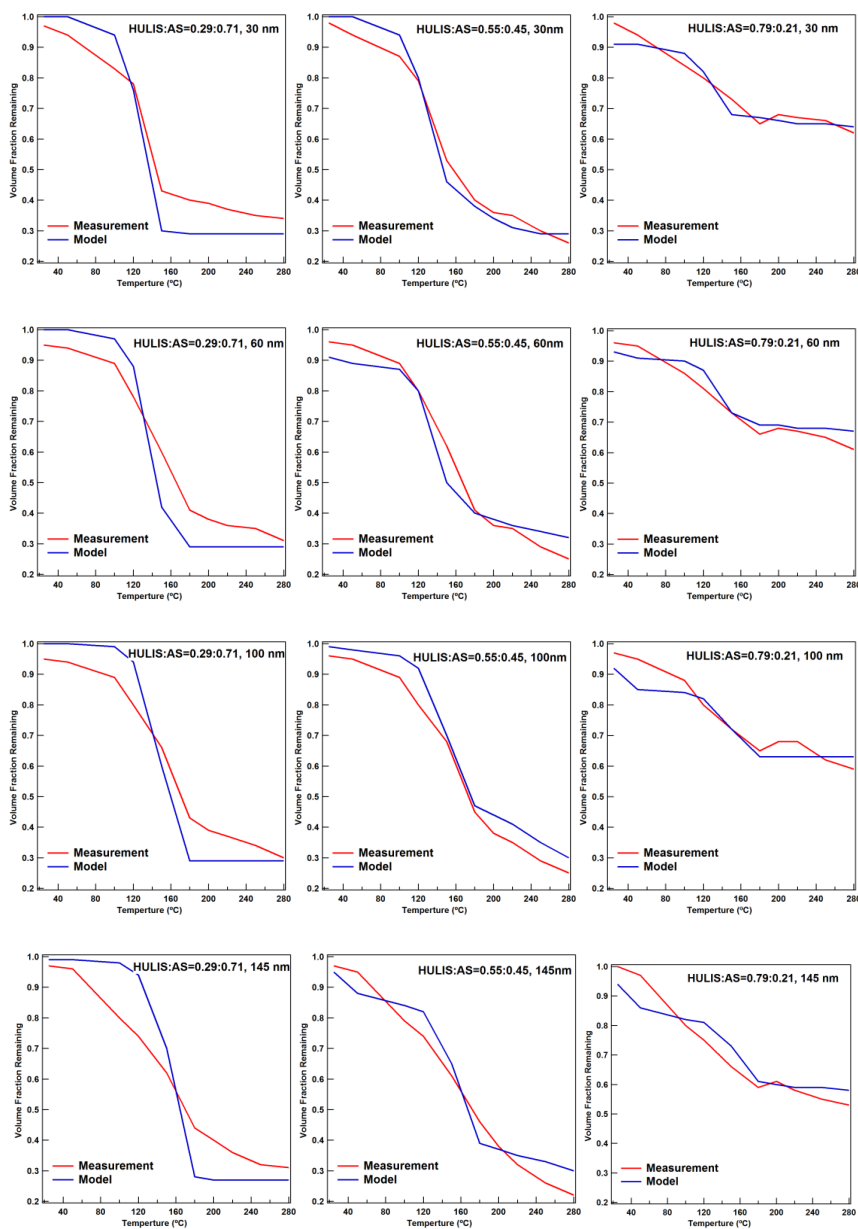


Figure 7 Measured and modeled volume fraction remaining (VFR) as a function of temperature for HULIS-AS mixed samples of 3 different mixing ratios at four different particle sizes of 30 nm, 60 nm, 100 nm and 145 nm

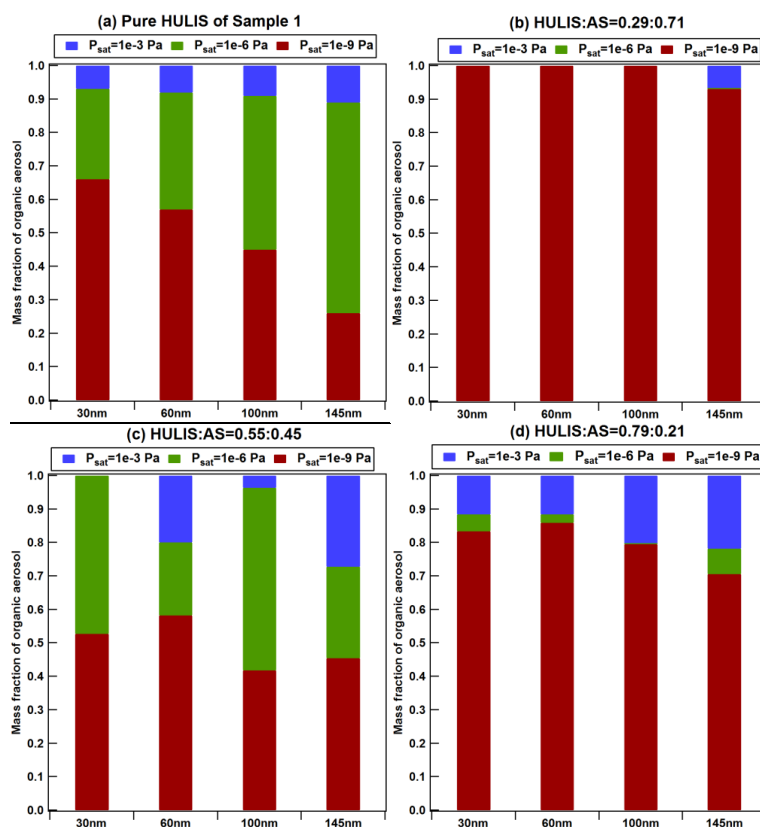


Figure 8 Model-derived mass fractions of organic compounds with different volatilities in four aerosol samples with different particle sizes of (a) 30 nm, (b) 60 nm, (c) 100 nm, and (d) 145 nm